ИНСТИТУТ ЯДЕРНОЙ ФИЗИКИ
им. Г.И. Будкера СО РАН

Bogdan B. Wojtsekhowski

PHYSICS ON INTERNAL TARGETS AT NEP RING

PREPRINT 92-20

НОВОСИБИРСК

PHYSICS ON INTERNAL TARGETS AT NEP RING

Bogdan B. Wojtsekhowski

Budker Institute of Nuclear Physics,
630090, Novosibirsk-90, Russia

ABSTRACT

Physics program presented here for nuclear physics studies by 200 MeV electrons, was developed by V. Dmitriev, I. Koop, D. Nikolenko, S. Mishev, I. Rachek, S. Popov, Yu. Shatunov, V. Telitsyn, A. Temnykh, E. Tsentalovich, D. Toporkov, V. Zelevinsky and myself during 1984 - 1987 for the physics motivation of the NEP ring construction. NEP project and its status are discussed also. Perspective physics program is shown. Pion photo production at threshold and elastic electron scattering on the polarized potassium 39 proposals are described in some details. Double polarized experiments for electro and photo nuclear reactions are unique possibilities at NEP.

INTRODUCTION

As well known internal target is a perspective new technique for nuclear physics studies. The idea and first demonstration of the superthin internal target regime were done in 1967 at INP [1]. New physics results were received at storage ring VEPP-2 and VEPP-3 [2 - 14].

The attractiveness of the internal target are:

- **Extremely high efficiency** using of the beam. Really, each electron pass through very thick target of 0.2 radiation length, which correspond $2\cdot10^{24}$ atoms/cm^2 (H_2).
- **Continuous generation** of the events characterized by frequency of RF system which is 8 Mc/s at VEPP-3, 52 at NEP and up to 3000 Mc/s at stretcher rings.
- **Transparency of the target** for recoil nucleus one of the unique features of the internal target. It will be used actively in threshold experiments and for investigations of the giant resonances decays.The mass of the material in the target is only 10^{-8} gram/cm^2 or less.
- **Unique target** of free neutrons in the magnetic trap is not

too thin for NEP. The limit of the neutron density is about 10^{16} particle/cm^3.

- **Wide class of pure polarizable targets** include H, D, ^3He, Li, Na, K and also N and some another.
- **Longitudinally polarized electron beam** become available in a storage ring. Additional advantage here is a very short time (20 ns for NEP) of the reverse of the polarization direction.

The Luminosity with external/internal targets useful to compare on the diagram (Fig. 1) suggested by Donnelly [15]. Today there is a possibility to show the positions of VEPP-3 and different projects on this plot. Additional light led by Figure of Merit of the experiment, which defined by luminosity, polarization of the target (beam), and detector solid angle.

For the finish of this short introduction let try to find the fields, where the internal targets fail? Today we can show only three such fields:

1. Extremely high luminosity experiments for Weak Interactions studies.
2. Unpolarized target experiments with high energy secondary particles.
3. Experiments with extremely high energy of the beam (higher than LEP energy).

Let me to describe attractiveness of the internal target from two another sides. They are:

i) polarized perspectives of the internal targets:

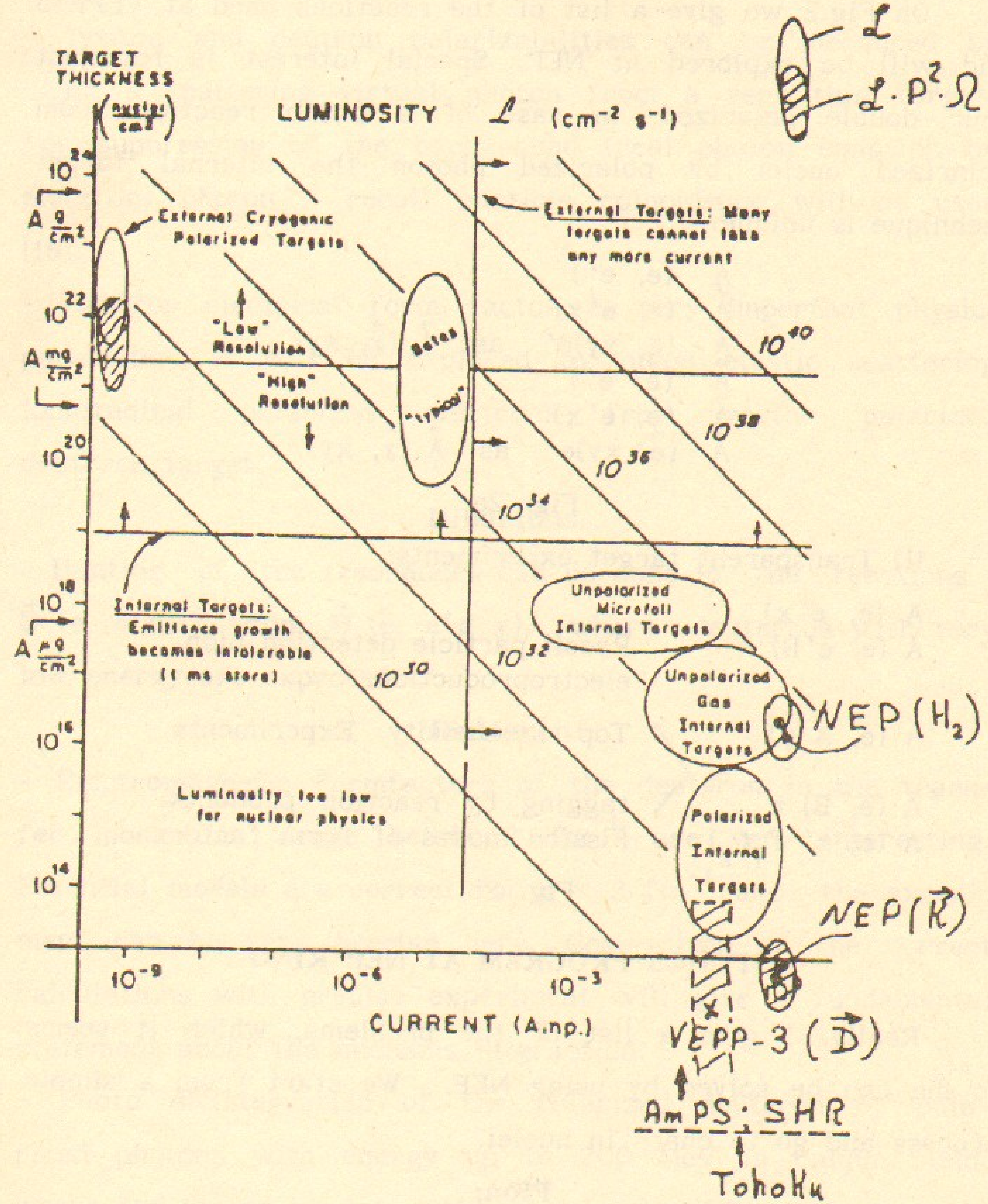

Fig. 1. Luminosity as a function of target thickness and electron current and Figure of Merit defined by luminosity, polarization of target (beam), and detector solid angle.

On Fig.2 we give a list of the reactions used at VEPP-3 and will be explored at NEP. Special interest is for last four double polarized. In case of a photo reaction from polarized nuclei by polarized photon the internal target technique is unique.

$\vec{A}$ (e, e′)
$\vec{A}$ (e, e′x)
$\vec{A}$ (e, xy)e′ as $\vec{A}$ ($\vec{\gamma}$, xy)
$\vec{A}$ ($\vec{e}$, e′)
$\vec{A}$ ($\vec{e}$, e′x)
$\vec{A}$ ($\vec{e}$, xy)e′ as $\vec{A}$ ($\tilde{\gamma}$, xy)

Fig. 2a.

ii) Transparent target experiments:

A (e, e′x)	
A (e, e′B) π	Recoil particle detection pion electroproduction.
A (e, A γ)	Top Luminosity Experiments
A (e, B) π	tagging by reaction products.
A (e, e′ $f_1 f_2$)	Fission modes of form factors.

Fig. 2b.

PHYSICS PROGRAM AT NEP RING

Really, I give a list of the problems, which it seems to me can be solved by using NEP. We start from a simple process and go to chaos in nuclei.

Pion:

- Long standing problem is a pion electroproduction near threshold and another one is the form factors of a negative pion production in the bound states.
- Coherent production of the pion on nuclei.

Nucleons:

- Proton and deutron polarizabilities can be measured by using a scattering virtual photon from a very thin target. For suppression of the background (real photon emission by electron) photon - recoil particle coincidence will be used [16].
- Neutron electrical form factor is very important physical parameter. It will be explored by quasi elastic scattering longitudinal polarized electrons from vector polarized deuteron target.

Dibarions:

- Hunting of the resonances can be done in the reactions $\vec{D}$ (e, e′d) π and $\vec{D}$ (e, e′d γ), where deuterons with very low energy are expected.

Deuteron:

- Electromagnetic Formfactors of the deuteron in the transfer momentum range below 2 fm^{-1} are very interesting. Potential models are correct for $q < 2\ fm^{-1}$ and the experiment can be very precise here. Comparison of the correct calculations with precise experiment will give a fundamental statement about the nucleons interaction.
- Photo disintegration of the polarized deuteron by polarized photons with energy up to 200 MeV is unique field, where the theory hope to predict and only NEP can to measure all parameters. The reactions are:

$\vec{D}$ (e, pn) as $\vec{D}$ ($\vec{\gamma}$, pn)
$\vec{D}$ ($\tilde{e}$, pn) as $\vec{D}$ ($\tilde{\gamma}$, pn)

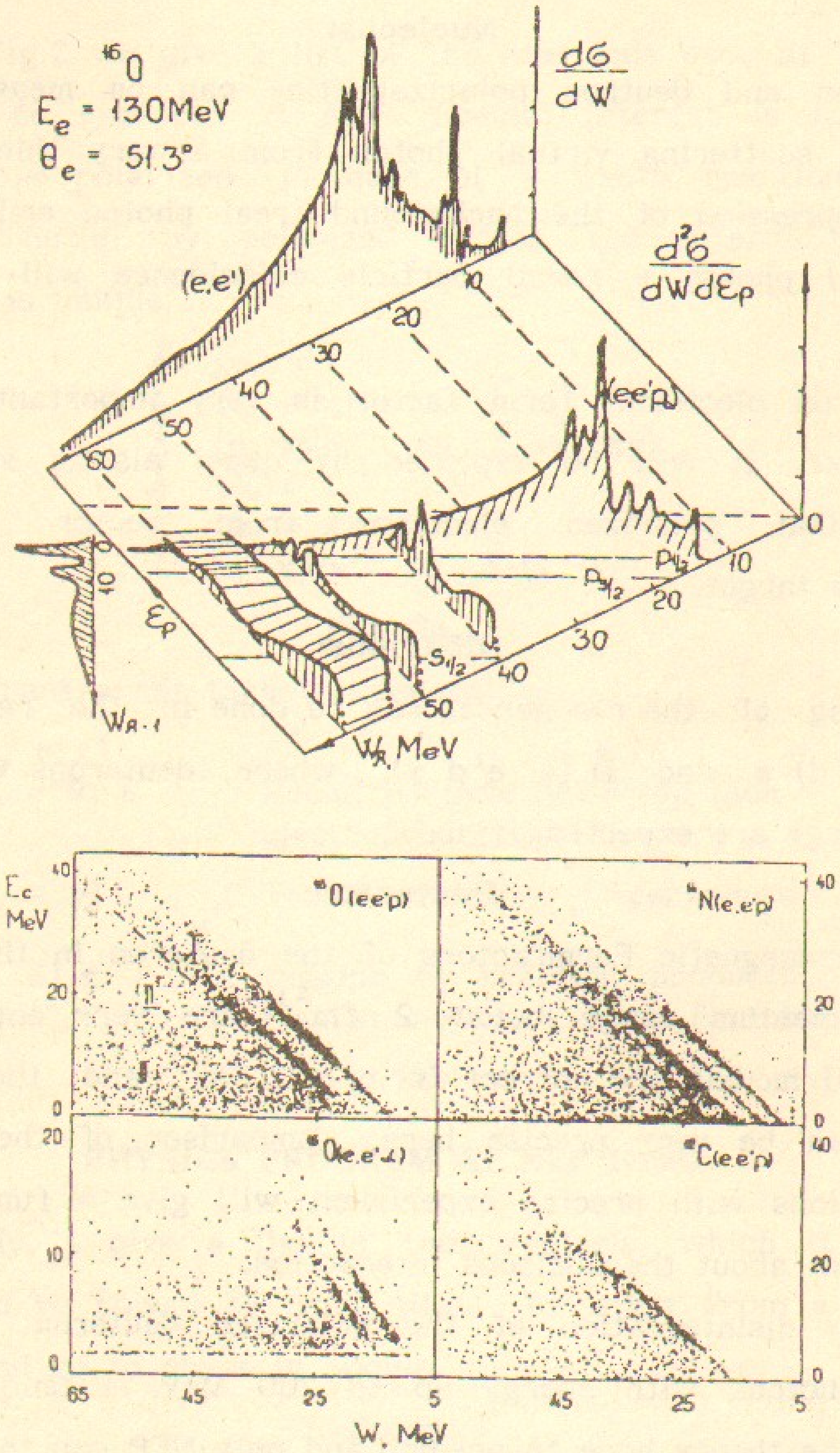

Fig. 3. Two dimensional presentation of the coincidence cross sections (e, e') and (e, e'x) reactions from ^{16}O.

- Electro disintegration of the polarized deuteron is new unexplored field, where investigation all structure functions is very important and difficult experimental task.

Nuclei:

NEP is the ring with energy range from 100 MeV up to 220 MeV was suggested mainly for Nuclear Physics studies. There is a wide program of the experiments, which can be divided on several parts:

a) Mechanism of the Reaction.
b) Giant Resonances.
c) Cluster effects.
d) Fission.
e) Quantum chaos kinetic.

I will present its details by using our results at VEPP-2.

Mechanism of the reaction inelastic electron scattering from nuclei is illustrated by two dimensional plots on Fig. 3. We hope to investigate following problems:

1. The role of 1p-1h configurations in dependence of the momentum transfer and excitation energy of nucleus.
2. Balance (e, e') and (e, e'x) cross sections. Previous result see on Fig. 4.
3. Photon inelastic process from nuclei in reactions (e,e'γ) and (γ, γ').

Well known results from Urbana showed the high efficiency of such method.

4. Multi particle emission mechanism in (e, e'xy) reaction.
5. Non quasi deuteron photo absorption above giant resonances region.

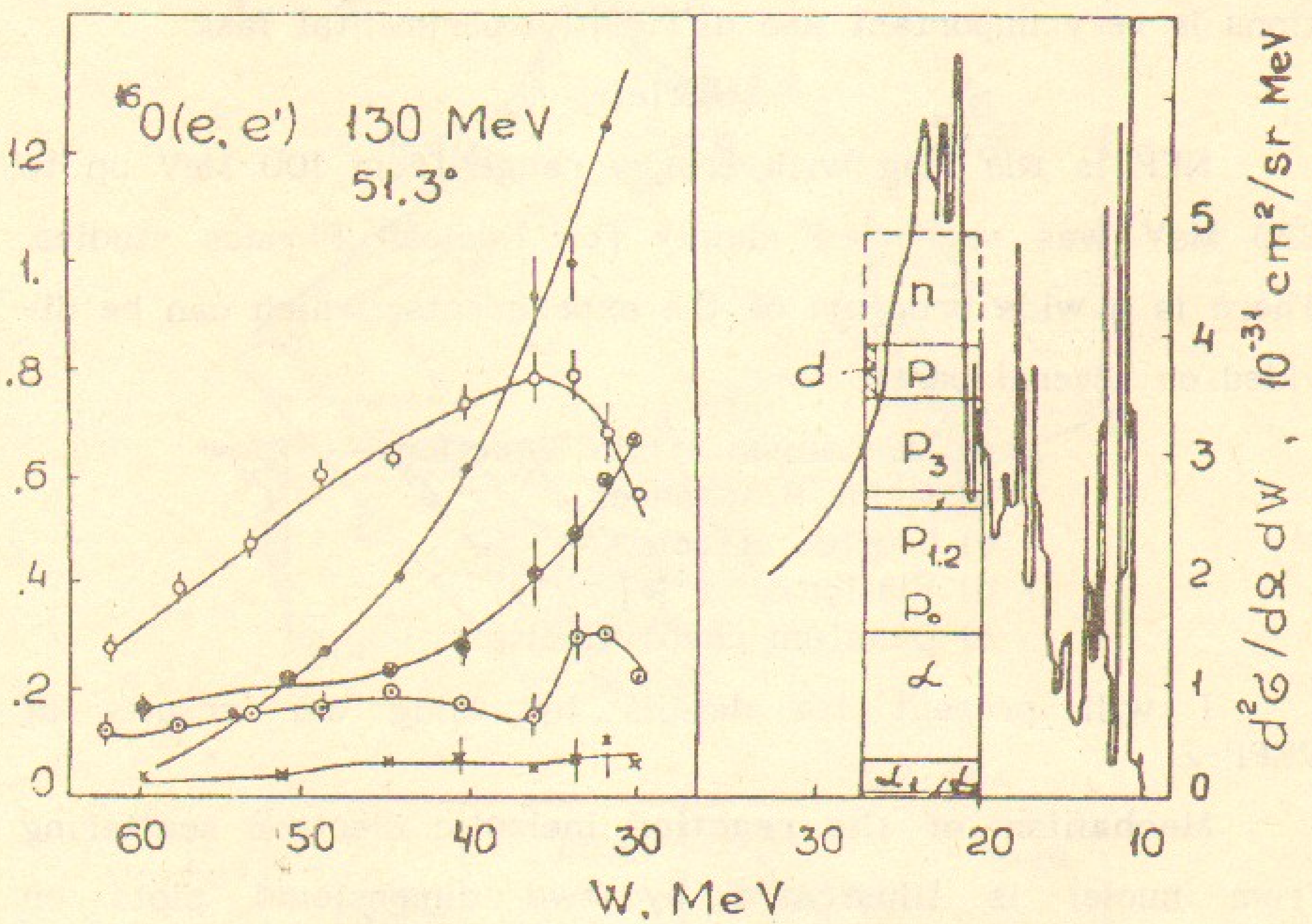

Fig.4. Balance of the cross sections $^{16}O(e, e')$ and (e, e′x) reactions: • - direct protons from 1p shell; o - isotropic proton emission; ⊙ - preequilibrium protons; × - anisotropic alphas; ⊗ - isotropic alphas.

The investigation of the last subject by circular polarized photon beam will be useful.

Giant Resonances Decays are the main collective phenomenons in the nuclei. Although they are explored during 30 years, the coincidence experiments start only few years ago. Many problems necessary to solved here:

1. Physical separation of the resonances and direct processes, multi pole decomposition; for example see Fig. 5;
2. Simple decay channels - p_0, n_0, α_0, γ_0; for example see Fig. 6;
3. Sum rule check separately for single multi pole force;
4. Alpha decay of the giant resonances;
5. Isospin mixing of the excited states;
6. Hunting of E0 resonances in light nuclei from (e, e′α) reaction by using of the alphas angular distribution;
7. Splitting of the giant resonances of deformed nuclei in $\vec{A}$ (e, e′x) reaction. This subject is very convenient for NEP, where will be unique polarized targets and low energy secondary particles can be detected.

Clusters in the nucleus also is long standing problem of nuclear physics. Very small thickness of the target is a large stimulus for search of the clusters.

1. Alpha clustering ((e, e′α) reaction and α/p ratio); our results on Fig. 7.
2. "Melting" of alpha associations on Tp(Wx), our results on Fig. 8.
3. Fission of the light nuclei: $^{32}S^{*} \rightarrow {}^{16}O + {}^{16}O$; for $^{24}Mg(e, f_1 f_2)$ see [17].
4. Knockout of clusters from heavy nuclei.
5. Alphas cascades; for example: $^{16}O^{*} \rightarrow {}^{12}C^{*} + \alpha \rightarrow 4\ \alpha$; our results on Fig. 9.

Fission by electrons is interesting in the comparison with one by proton and heavy ions. The transparency of the target give possibility to investigate following problems:

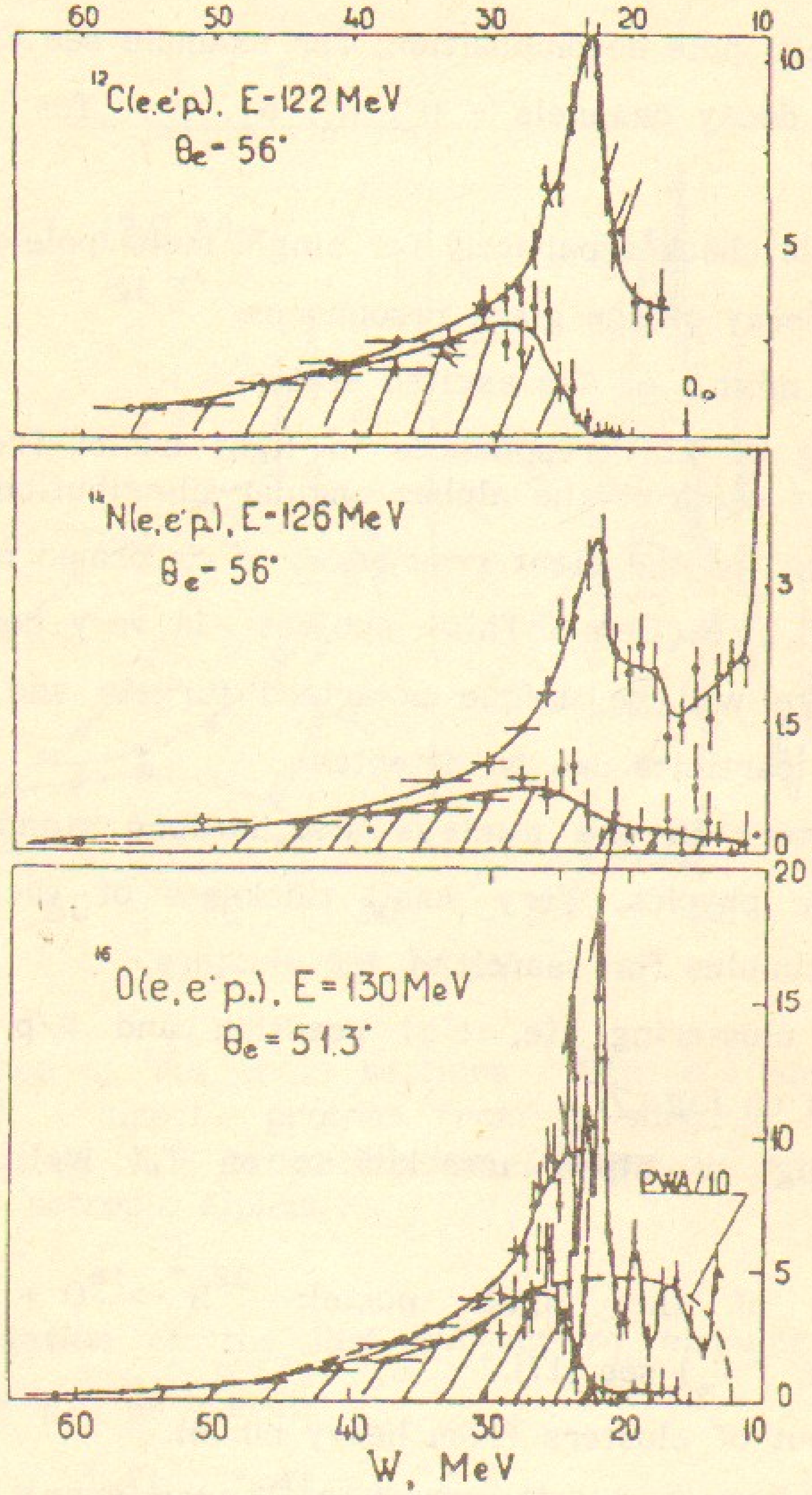

Fig. 5. Decomposition of the (e, $e'p_0$) cross section as an asymmetrical part ("quasi elastic" - dashed area) plus E1 resonance.

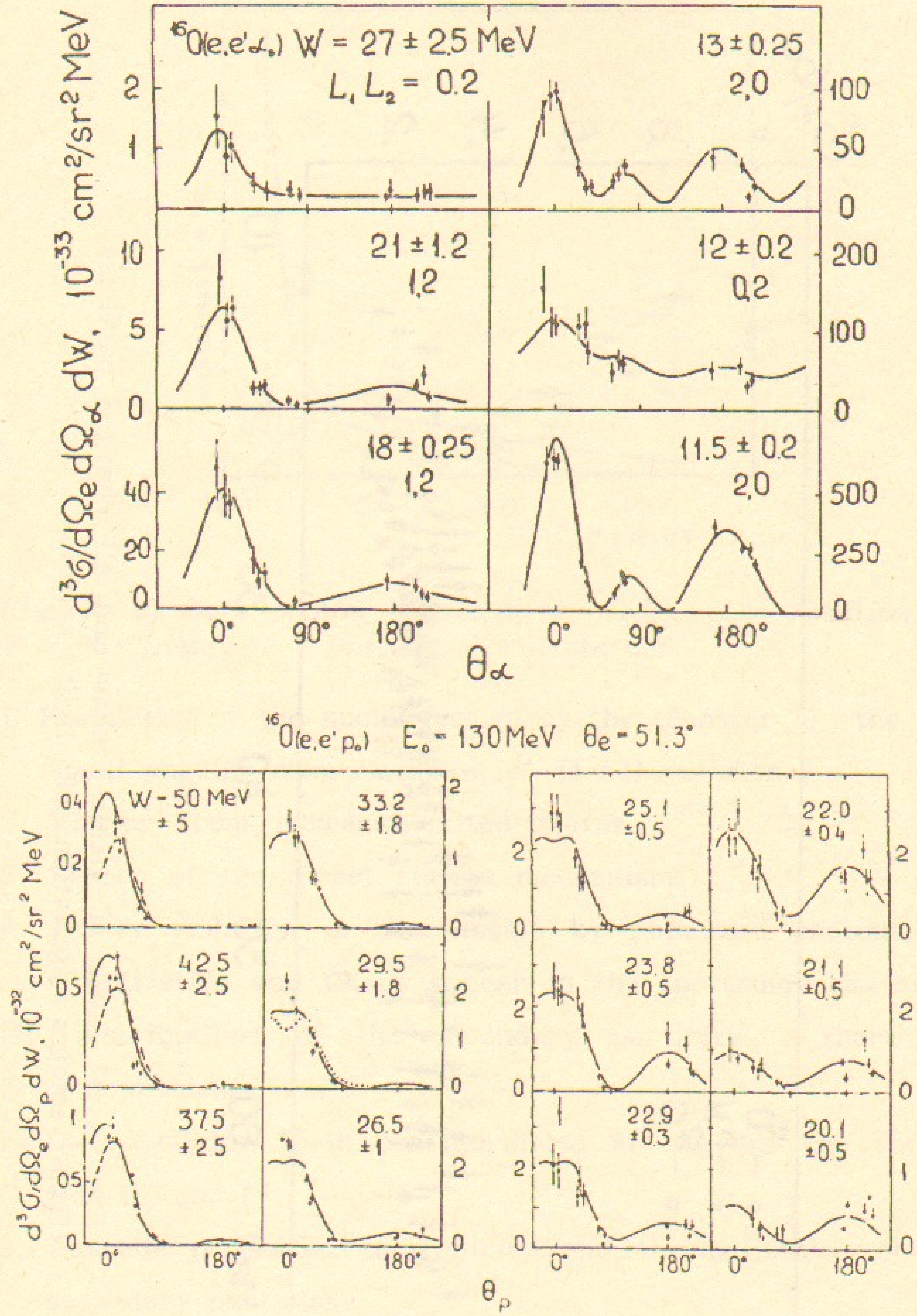

Fig. 6. Angular distributions for $^{16}O(e, e'p_0)$ and $(e, e'\alpha_0)$ reactions.

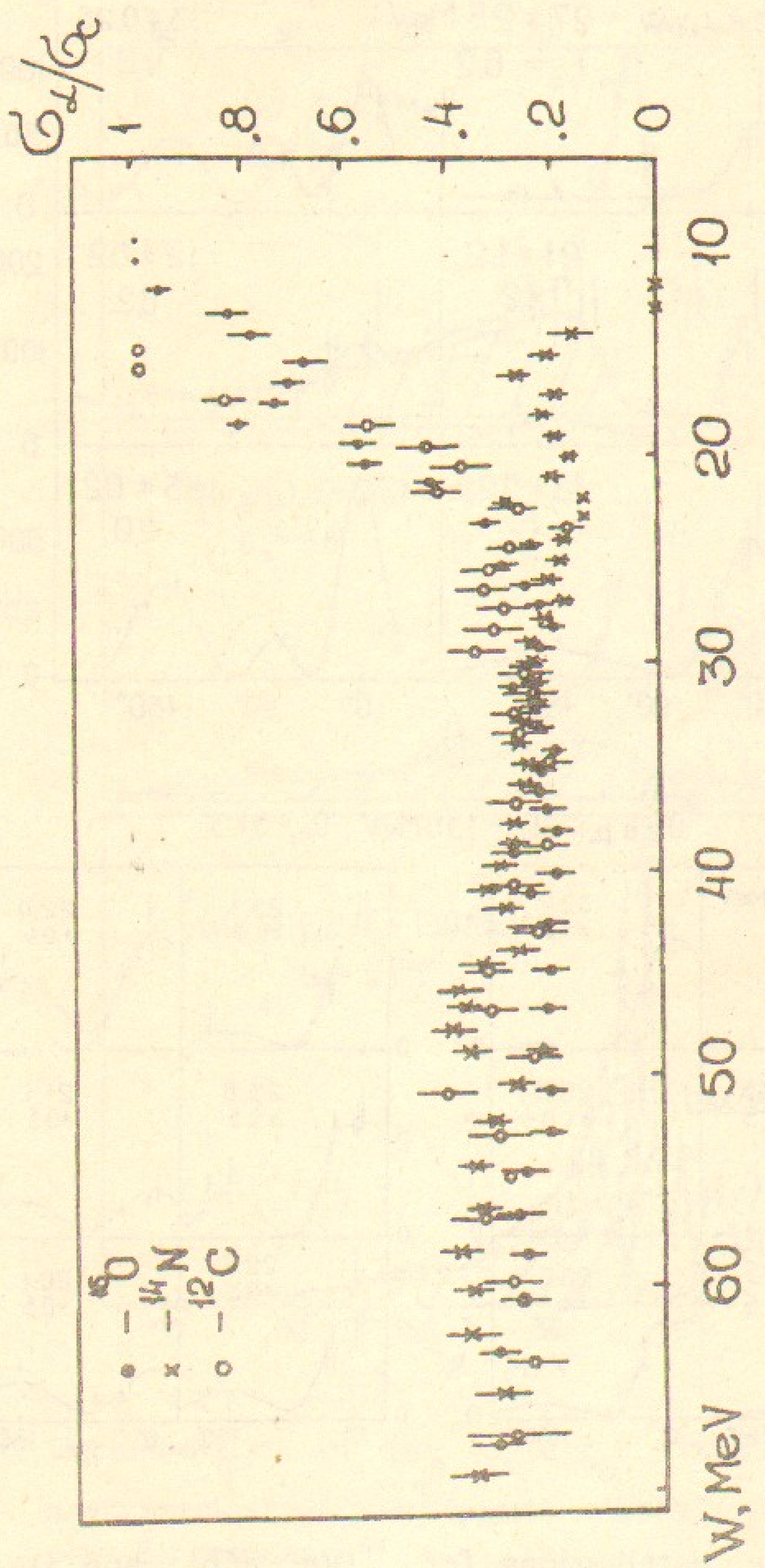

Fig. 7. a) Ratio of yields alphas and all charged particles from electro excitation of light nuclei.

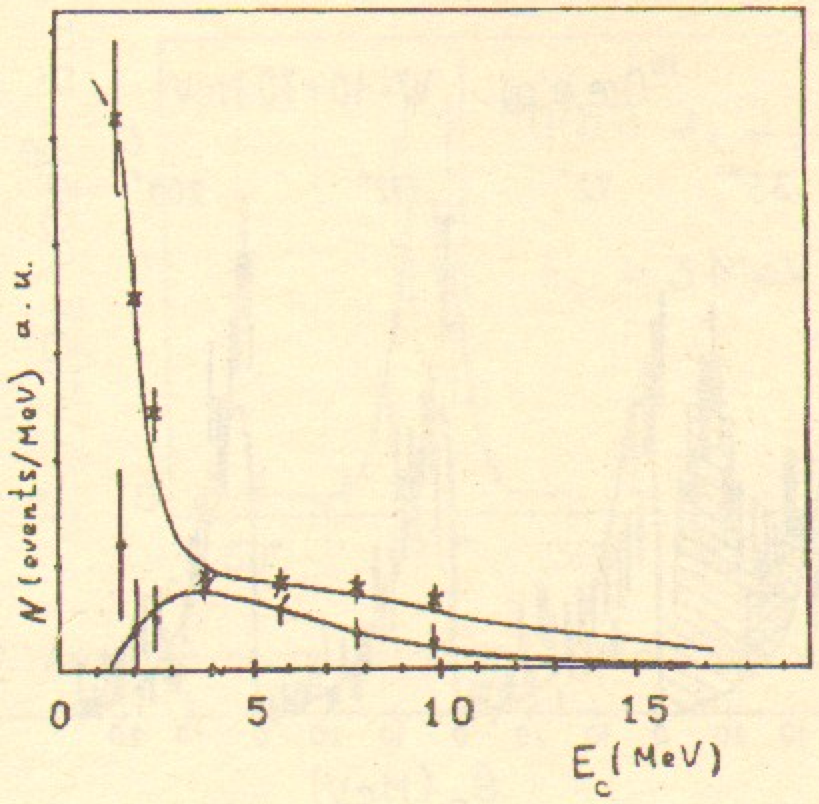

Fig. 7. b) Soft proton emission in $^{14}N(e, e'c)$ reaction for W_x = 35÷70 MeV, x - protons, o - deuterons.

1. Feasibility of the nuclei fission by the transfer of the small angular momentum: (e, e′ f1 f2) reaction.
2. Fission from isomeric exited states.
3. Search of the direct fission mechanism.
4. Parity violation in the fission by polarized photons.

Statistics and Chaos appear in the spectrums and angular distributions of the secondary particles. There are several problems here:

1. Decay of the 1p-1h configuration; kinetics of the formation $\Gamma_\uparrow$ and $\Gamma^\downarrow$.
2. Cascade processes, multiplicity and thermalization of the secondary particles.
3. Statistical effects in the density of nuclei exited states.

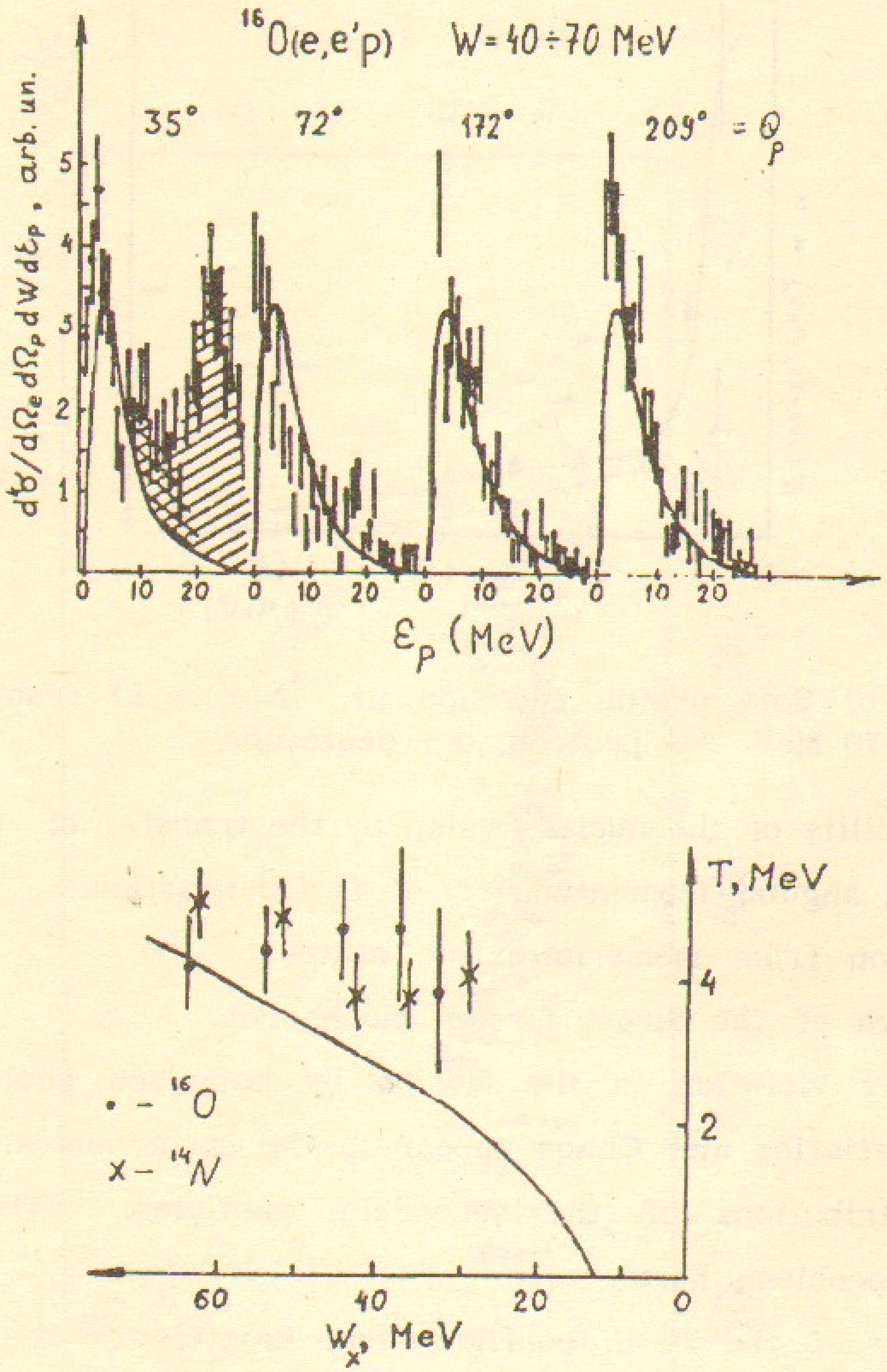

Fig. 8. Proton spectrums for different emission angles from $^{16}O(e, e'p)$ reaction and "temperatures" of the protons from isotropic proton emissions of ^{14}N and ^{16}O.

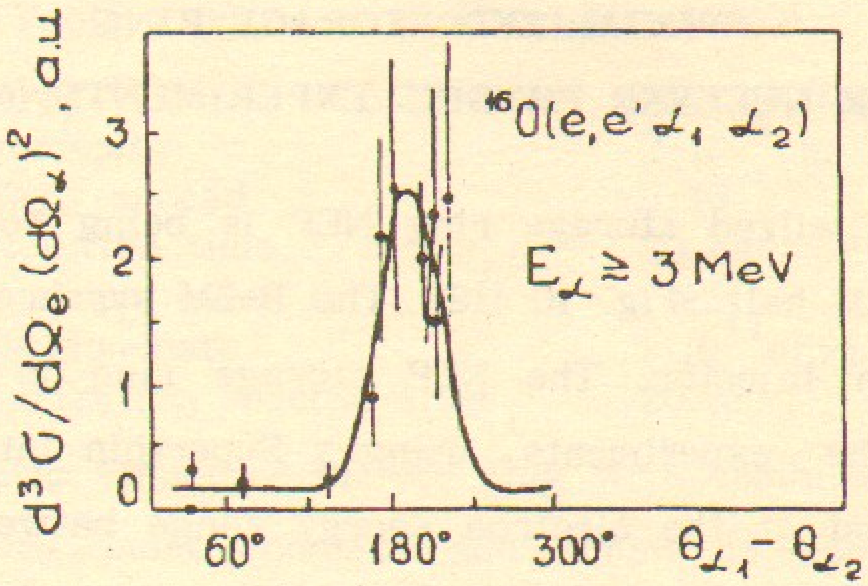

Fig. 9. Angular correlation in $^{16}O(e,e'\alpha\alpha)$ reaction.

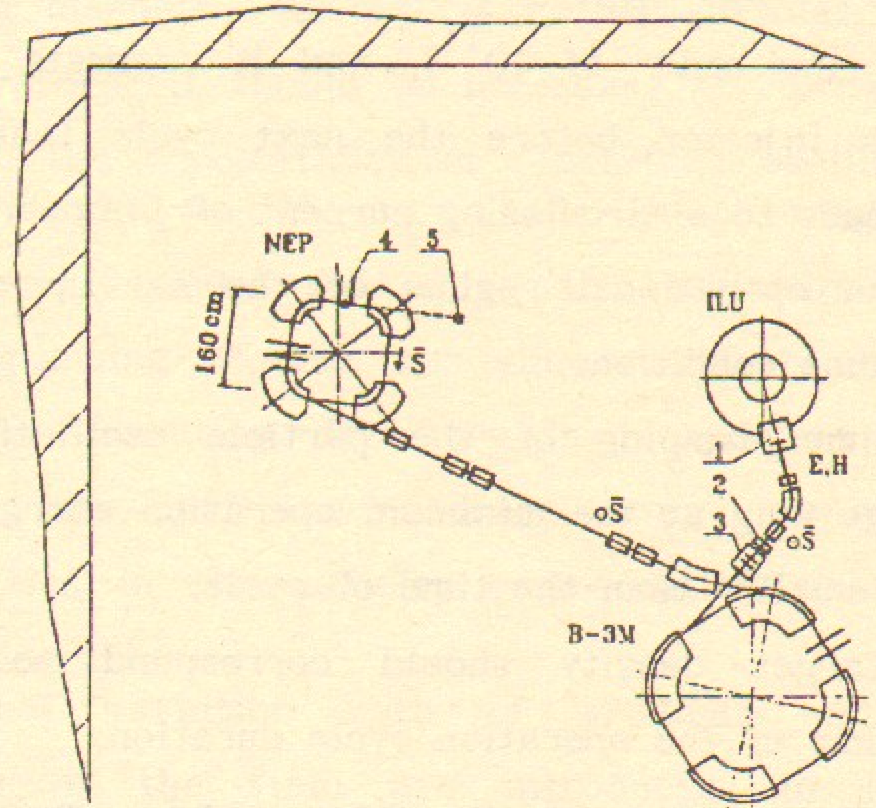

Fig. 10. Scheme of NEP polarized electron project: 1 - source with AsGaP photocathode; 2 - Mott polarimeter; 3 - linear accelerator; 4 - flipper; 5 - Compton polarimeter.

SPECIALIZED STORAGE RING FOR NUCLEAR PHYSICS EXPERIMENTS (NEP)

A specialized storage ring NEP is being constructed at the VEPP-2M hall -Fig. 10 [18]. The B-3M synchrotron will be used as an injector. The NEP storage ring is designed to perform the experiments using a Superthin Internal Target (SIT) method at the electron energy range between 100 and 220 MeV. Timing operation cycle of the set up is adjusted to parameters of the B-3M synchrotron (the repetition frequency of the injection pulses is up to 2 Hz, the maximum energy is up to 250 MeV, the number of particles in the pulse being of the order of 10^{11}), and it suggests the use of all particles injected before the next cycle (particle number corresponds to a circulating current of 1 Ampere).

Such an operational regime of the set up requires, in particular some conditions:

i) the time damping of the particle oscillations in the storage ring at the minimum operation energy should be much smaller than the time of cycle;

ii) the target density should correspond to the beam life time of the operation cycle duration;

iii) the beam transverse sizes and energy spread, established due to the interaction with a target, should be much smaller than the respective storage ring admittance (superthin target regime).

Table 1. Physical parameters of NEP

Energy	100-220 MeV
Luminosity	$2\cdot10^{35}$ cm^{-2}/s (H)
Energy spread	$3\cdot10^{-4}$
Revolution time	20 ns
Beam spot size	1 mm
Injection rate	$1\cdot10^{11}$ el./s
Polarization reverse time	20 ns

A magnetic structure of the ring with combined focusing is chosen being most compact and simple in operation. To provide a minimal damping time, field is taken close to the limiting one for iron (18.3 kG). The relation between the length of the straight section (80 cm) and the curvature of the orbit in magnets (40 cm) is rather unusual, it is very large. Therefore, it should be necessary to provide a compensation of the chromaticity of betatron oscillations with tunes equal to $\nu_x = 1.15$, $\nu_z = 1.13$ (the average magnetic field index n is equal 0.5 along the orbit in a magnet). Further lengthening of the straight section to improve the conditions for inserting detectors is inexpedient because it results in loss of the storage ring admittance and new difficulties in chromaticity compensation to achieve the desired compensation.

Azimuthal variation both of gradient and quadratic non-linearity of the field are introduced. In the central part of the magnet along the azimuth a field index n = 0 and H" = 41 G/cm^2, and in symmetric edge sectors n = 1 and H" = =-30 G/cm^2. The magnet gap is taken equal to 4 cm, the radial aperture used for the beam storage is ± 2 cm. A comparatively large (5%) energy acceptance of the storage ring is required to provide the optimal operation regime with an internal target.

Table 2. Storage ring parameters

Energy	100-220 MeV
Bending radius	400 mm
Revolution time	20 ns
Damping betatron oscillation time	22 ms
Field strength	18.3 kG
Length of straight section	820 mm
Vertical aperture	36 mm
Radial aperture	40 mm
Field index	0.5
Betatron frequencies	1.15 (1.13)
Synchrotron frequency	$3.5\cdot10^{-3}$
Resonator voltage	20 kV
Injection: pulse channel elements -	1 ms
pulse iron magnet -	0.08 ms
pulse one turn magnet -	40 ns

NEP luminosity for different Z targets and beam energy is given in Table 3.

Table 3.

Z_{target}	1	8	20	50
E_e = 120 MeV	1.9 $\cdot10^{35}$	1.1 $\cdot10^{34}$	2.3 $\cdot10^{33}$	4.5 $\cdot10^{32}$
E_e = 200 MeV	2.2	1.4	3.0	5.8

The thickness of the hydrogen and oxygen targets for maximum luminosity are $3\cdot10^{16}$ atom/cm^2 and $2\cdot10^{15}$ atom/cm^2.

Polarized beam is a crucial element of the NEP program. At first glance, it seems impossible to use polarized longitudinally electrons to carry out experiments with an internal target in a ring accelerator, since electron spin is precessing since the gyromagnetic ratio is not exactly equal to two. Spin-Flip methodic [19] provides the solution both problems: the transformation direction of polarization from vertical to the orbit plane and the increase of the beam depolarization time by some orders as compared to the free precision case.

The NEP storage ring will make use of a polarized source similar to the SLAC design. The vertical polarization required by the B-3M synchrotron will be produced by a WEIN filter in the channel between the source and ring accelerator. The spin resonance $\nu_z = 1 - \nu$, where ν_z is the vertical betatron frequency and ν is spin frequency occurs at 45 MeV. The depolarization in crossing this resonance will be small because of the high rate of acceleration. The resulting vertically polarized beam will then be injected into NEP.

The idea of controlling the polarization in the storage ring makes use of the small spread in spin tunes. This idea is realized by using a weak Radio Frequency (RF) field [19]. The spin tune is $\nu = \gamma\cdot\mu'/\mu_0 = E_e(\mathrm{MeV})/440.7$, where μ' and μ are anomaly and Dirac magnetic moments. According to [20], the spread of spin tunes is given by: $d\nu/\nu = \lambda/R\cdot\gamma^2/\nu_x^2$, where λ is Compton length of electron, R is bending radius. This formula produces a good estimation, when $\gamma\cdot d\nu_x/d\gamma \approx 1$. For NEP ring, R = 40 cm, γ = 440, so that available value $d\nu/\nu$ is about $2\cdot10^{-7}$!

It is useful to consider the spin dynamics in a coordinate system rotating around the vertical axis at the RF frequency ω. The detune ε from spin resonance ν, is given by: $\varepsilon = \nu - \omega + m$, which reflects the magnetic field seen in the rotating coordinates. The RF field may be described in arbitrary units by the amplitude of resonance component of the RF field:

$$w = (0.5 \cdot B_{RF} \cdot l_{RF}) / (B_{bending} \cdot 2 \cdot \pi \cdot R) .$$

Since the time variation of γ is much slower than the spin precession in both the lab and rotating coordinate systems, the equation for spin motion may be written as: $d\vec{S}/dt=[\vec{h}\times\vec{S}]$, where $\vec{h} = \vec{\varepsilon} + \vec{w}$. As result the projection S_h is an integral of the motion. By adiabatically changing h we can change the direction of $\vec{S}$, while conserving the value of S_h.

The depolarization rate is due to jumps of γ by synchrotron radiation that produce fluctuations in ε and the diffusion of spins of individual particles. According [20], the depolarization time is $\tau_d = \tau_0 \cdot (w/d\nu)^2$, where τ_0 is the damping time.

After injection of the beam and damping of the beam oscillations, the Radio Frequency solenoid (flipper) switched (see Fig. 11). It produce a magnetic field about 20 Gs in length 40 cm directed along particles velocity. Flipper will be switched on with detuning ε_i from the spin resonance. The value ε_i must be less than the frequency of the synchrotron oscillation $\nu_s = 3 \cdot 10^{-3}$ and and much more than $w \approx 10^{-4}$. Than, the flipper detuning ε will be changed adiabatically to the resonance one. The

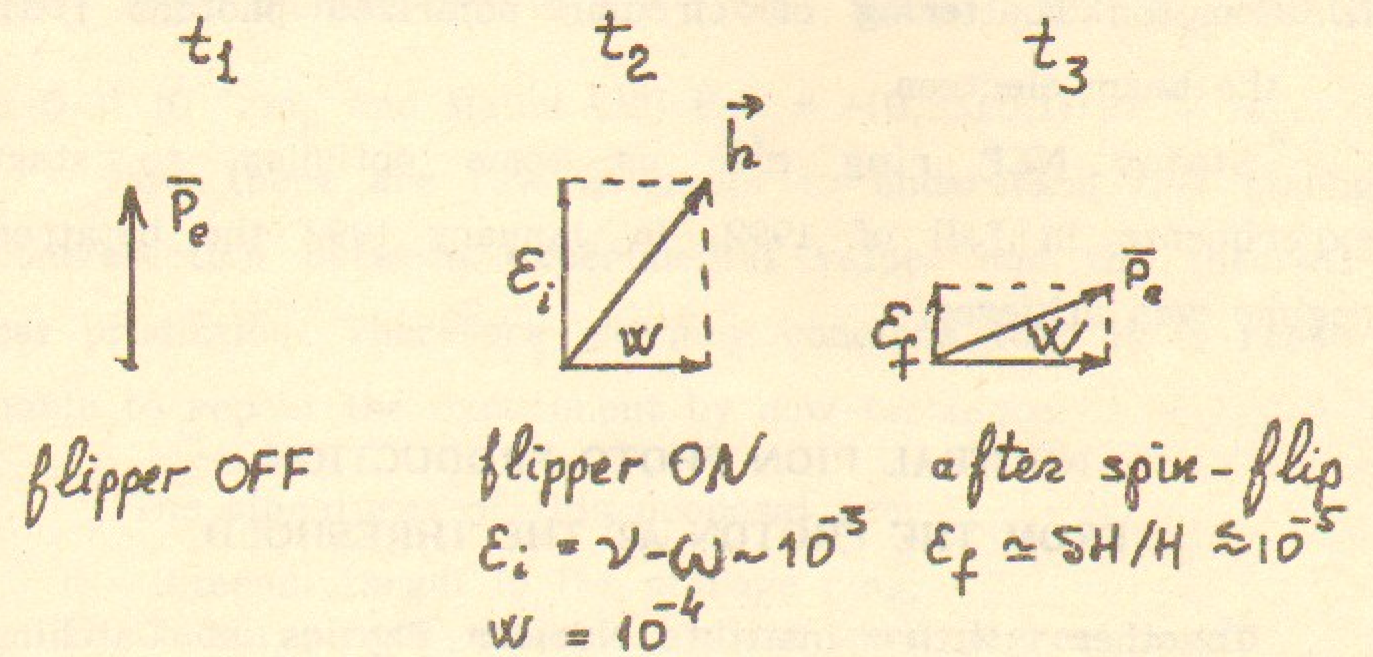

Fig. 11. Principle of operating with the flipper for transformation vertical polarization to orbit plane.

final ε_f actually determined by the instability of the NEP magnetic field and can be less 10^{-5}. After 90 degree flip of the spin to the orbit plane the detuning ε will be fix about zero. The flipper "become" a guide and save a degree of the polarization during long time. For NEP parameters the RF power of the flipper will be about 5 kW and available depolarization time is more than one hour. If for experiments used a beam with energy 220 MeV the direction of spins will be flip every turn (20 ns). For typical beam life time 1 - 2 second a false asymmetry of the experiment will be reduced by factor $\tau_d/t_{turn} = 10^8$.

For measuring the degree of the electron longitudinal polarization two methods will be applied:

i) scattering of beam electrons from polarized electrons of a hydrogen target;

ii) Compton scattering of circular polarized photons from the beam electron.

Status NEP ring give us some optimism to start experiments in fall of 1992. In January 1992 the betatron regime was achieved.

NEUTRAL PION PHOTO PRODUCTION FROM THE PROTON AT THE THRESHOLD

Together with Institute Nuclear Physics at Gatchina (V. Nelubin) we proposed the scheme of the measuring the differential cross section of the neutral pion photo production from the proton at forward and back c.m.s. angles near the threshold. The high intensity electron beam of NEP storage ring will used together with internal hydrogen target. The purpose of the experiment proposed is the investigation of the energy dependence of the S-wave photo production amplitude E_{0+} near the threshold. This amplitude is defined by the relation:

$$\frac{k}{q}\cdot\frac{d\sigma}{d\Omega}\Bigg|_{q\to 0} = |E_{0+}|^2,$$

where q is pion and k is photon momentum.

Electric amplitude E_{0+} is the fundamental quantity in physics of the strong interactions for which the Low Energy Theorem (LET), basing on current conservation and approximate chiral symmetry, predicts [21] $E_{0+}(\mathrm{LET}) = -2.4\cdot 10^{-3}/m_\pi$.

The experimental results are from Saclay [22] $E_{0+}=-(0.5\pm 0.3)\cdot 10^{-3}/m_\pi$ and Mainz [23] $E_{0+} = -(0.35\pm 0.1)\cdot 10^{-3}/m_\pi$.

Now there are few attempts to understand this strong contradiction between experimental values and the theoretical prediction. Therefore we may conclude that it is reasonable to repeat the experiment by new technique.

The signatures of this proposal are:

i) internal target in the storage ring;
ii) recoil proton detection about zero degree in lab system;
iii) reconstruction of the initial photon energy by value of proton energy;
iv) no photon tagging and, as result, a high luminosity of the experiment;
v) almost $4\cdot\pi$ detection geometry near the threshold.

Fig. 12 shows the kinematic plot of the proton energy dependence on its out coming angle in lab system for the different initial photon energies. In order to obtain the initial photon energy it is necessary to measure the recoil proton energy only. It should be emphasized that the relative small angle acceptance near 0^0 in lab system provides the full acceptance in c.m.s. at the threshold.

The 170 MeV electron beam crosses through the internal hydrogen target- Fig. 12. The recoil protons which are produced at the 0^0 angle as the result of the equivalent photons interaction with the target protons pass through the bending magnet and are detected. The led glass detectors will be used for registration of γ-rays from the π^0-decay to

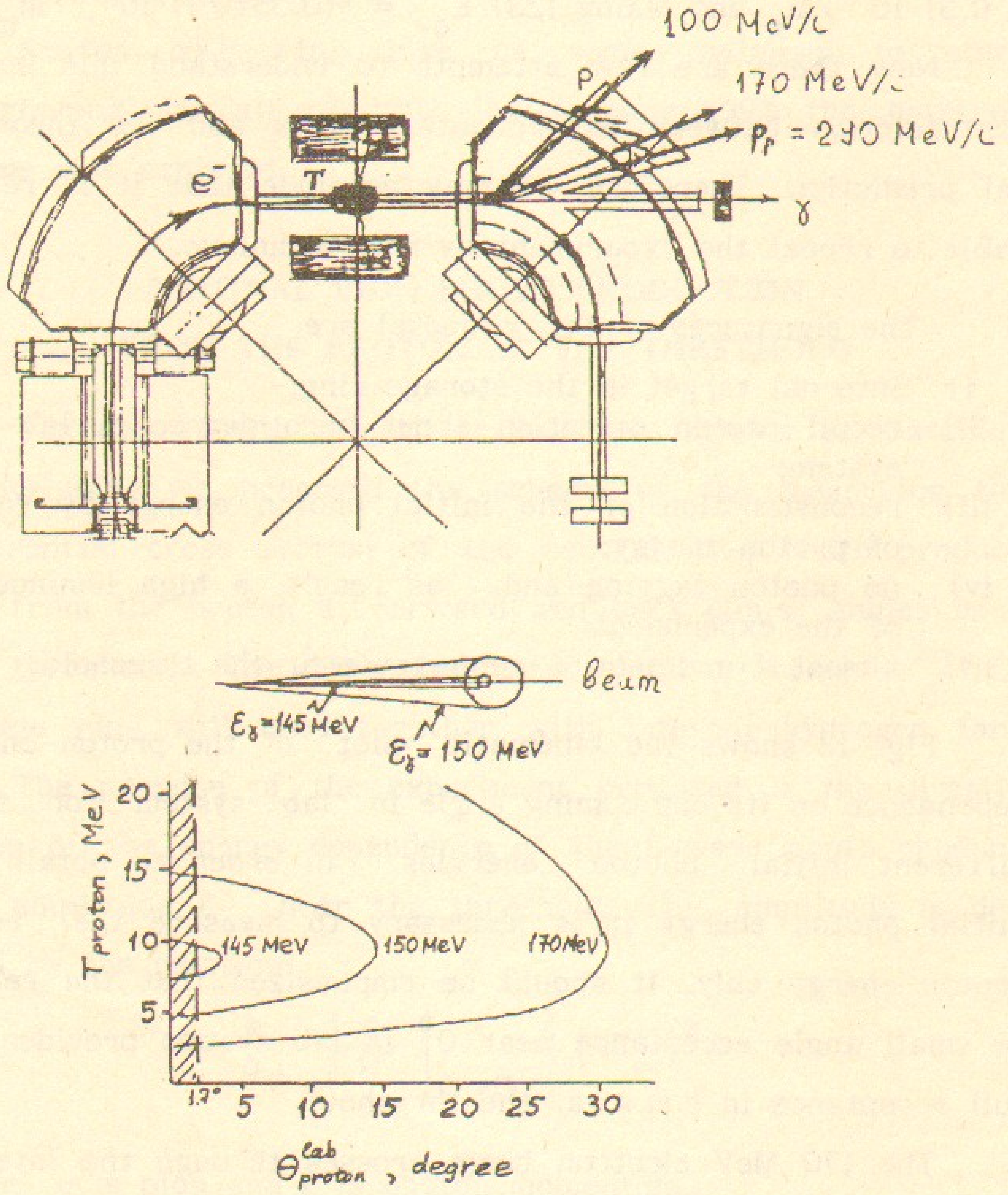

Fig. 12. Layout of the experimental setup for neutral pion photo production and energy - angle correlation for recoil protons.

reduce the background from the tail of e p-elastic scattering. The measurement of the recoil proton from e p-elastic scattering will be used as a monitor process. The main parameters of this experimental setup are as follows: the electron beam intensity is one Ampere; the target thickness is about $3\cdot10^{16}$ atoms/cm^2; the recoil proton angular acceptance is from 0^0 up to 1.7^0; the luminosity $\mathcal{L}$ per one MeV is about 10^{31} cm^{-2}/s.

Under such conditions it is possible to obtain the statistical accuracy about 10% in one MeV bin of the photon energy during a few days run.

ELASTIC ELECTRON SCATTERING FROM POLARIZED POTASSIUM 39

Together with NIKHEF-K at Amsterdam (C. de Jager and H. de Vries) we are preparing experiment for separation of the magnetic dipole and octupole form factors. From unpolarized experiments only sum of M1 and M3 is known. On Fig. 13 from reference [24] shown the experimental form factor and theoretical predictions. The cross section of the elastic scattering of the unpolarized electrons from polarized nuclei with spin 3/2 can be present as:

$$d\sigma/d\Omega = \Sigma_0\cdot(1+R_2^0(q,\vartheta)\cdot P_2(\cos\vartheta^*)+R_2^1(q,\vartheta)\cdot\cos\varphi^*\cdot P_2^1(\cos\vartheta^*)+$$
$$+\ R_2^2(q,\ \vartheta)\cdot\cos2*\varphi^*\cdot P_2^2(\cos\vartheta^*))$$

where Σ_0 is unpolarized cross section, q is transfer momentum, ϑ is electron scattering angle, ϑ^* and φ^* are describe the polarization direction, $R_j^i(q,\ \vartheta)$ are functions

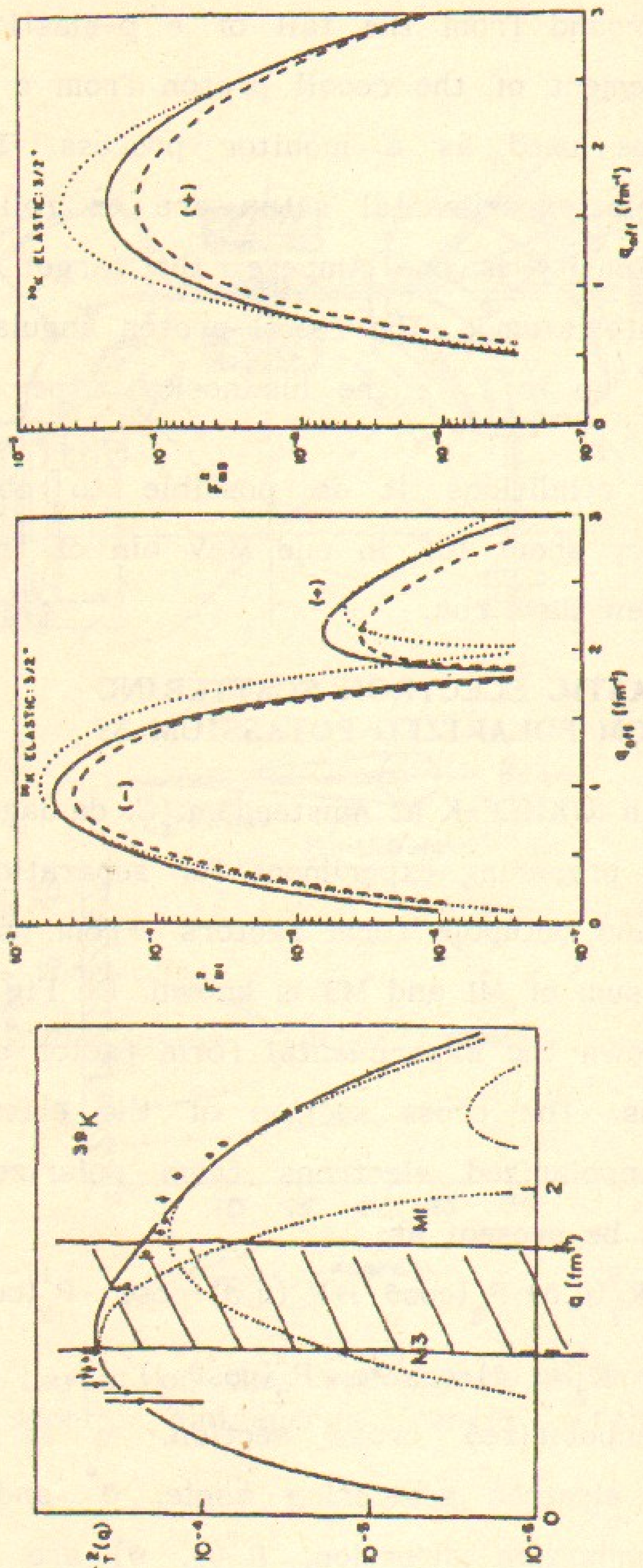

Fig. 13. The experimental form factor F_T^2 and theoretical predictions for F_{M1}^2 and F_{M3}^2 of ^{39}K.

of the nucleus form factors F_{C0}, F_{C2}, F_{M1}, and F_{M3}. The sums of the form factors (F_L^2 and F_T^2) are measured in the unpolarized experiments. Appropriate choice of the polarization direction ($\vartheta^* \approx 55^\circ$, $\varphi^* = 90^\circ$) reduce number of unknown parameters to F_{M1} and F_{M3} in a function

$$R_2^2(q, \vartheta) = f_2/5\ (F_{M1}^2 - F_{M3}^2 + F_{M1} \cdot F_{M3} / \sqrt{6})/F_\Sigma^2 ,$$

where f_2 is Fano tensor, $f_2 = (n_{3/2} - n_{1/2} - n_{-1/2} + n_{-3/2})/2$ and n_i are occupation numbers of the magnetic sub levels of the target nuclei. The scheme of the experiments presented on Fig. 14. Holding magnetic field is mainly vertical with small horizontal component along the beam direction. Such choice of the field direction suitable for storage ring operation.

Characteristics of the experiment are:

i)	transfer momentum range	1.0 up to 1.5fm^{-1};
ii)	electron current in the storage ring	1 Ampere;
iii)	target thickness (length 4 cm)	10^{13} atoms/cm;^{2}
iv)	target polarization	100%.

The run time required for 10% accuracy determination of F_{M1} (time T_1) and F_{M3} (time T_3) given on Fig. 15 for different angles of scattered electrons (calculated by A. Volosov). We are planning to connect a storage ceil and a pumping cell by short tube with largre diameter. As result required density of polarized potassium will be achieved without any radiation trapping problems.

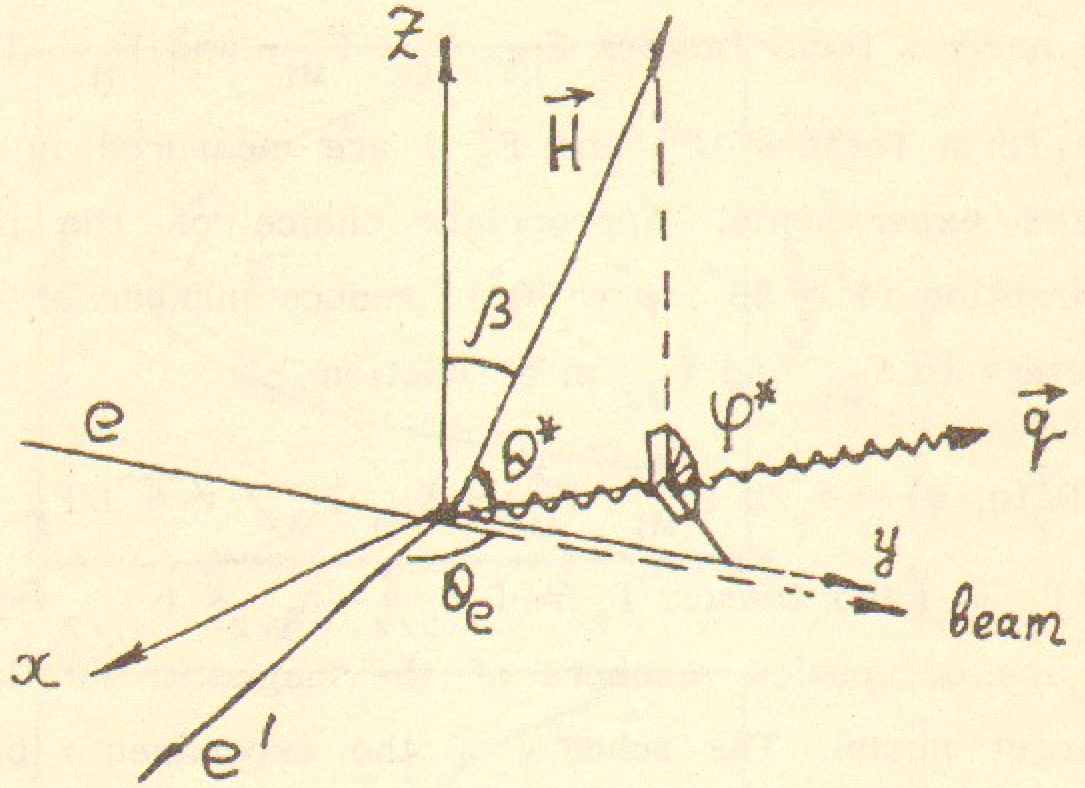

Fig. 14. The geometry of the electron scattering from polarized nuclei.

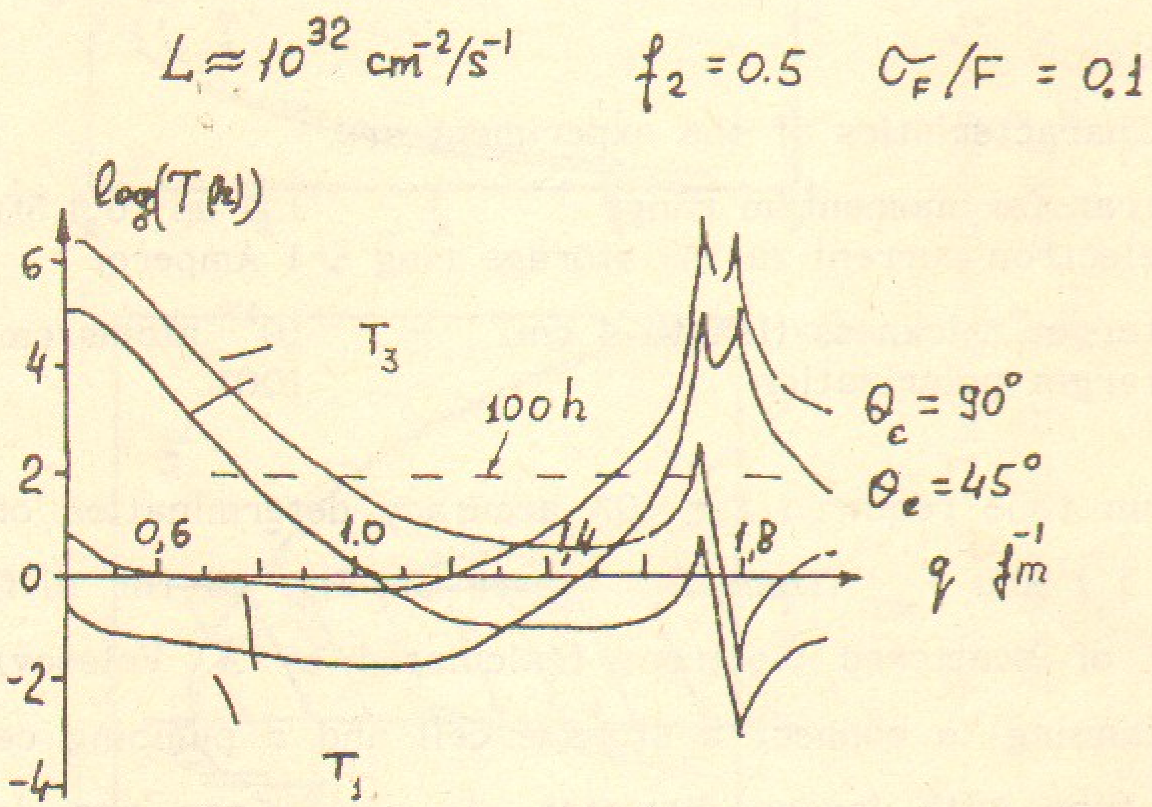

Fig. 15. Run time for 10% accuracy of the measurement of the magnetic form factors.

DOUBLE POLARIZED PHOTO PRODUCTION EXPERIMENTS AT STORAGE RING

Experiments on virtual photons by using internal electron beam in storage ring were began from deuteron polarized target at VEPP-2 [12]. The control of the photon q_μ^2 was done by measuring parameters of the secondary particles. Similar idea was suggested [16] for measuring Compton effect on proton by using virtual photons. Additional information about photon induced reactions can be obtained if to determine the electron scattering plane (by its reconstruction from secondary particles momentums). As result, will be obtained data for electrodisintegration at low q_μ^2. The azimuthal variation of the cross section, according [24], is $\cos 2\varphi \cdot v_{TT} \cdot R^{TT}$ and give information about linear polarized photon asymmetry. The experiments on circular polarized virtual photons much more simple, because the degree of polarization defined by longitudinal polarization of electrons and the ratio of the photon and electron energies. In both cases (linear and circular) the high polarization of the internal targets made virtual photon technique very perspective.

CONCLUSION

Electromagnetic spin physics has excellent future with Superthin Internal targets in storage rings. For full scale experiments it is necessary to have high current specialized rings in wide energy range from 100 MeV (it is NEP) up to several GeV. I would like to thank the organizers of the conference on Electromagnetic Physics at Storage Rings in December 1991, Sendai, Japan for kindness and support.

REFERENCES

1. *G.I. Budker at al.* Yad. Fiz., vol. 6 (1967) 775.
2. *S.T. Belyaev, G.I. Budker, S.G. Popov.* Proceeding 3-th Intern. Conf. on High energy physics and nuclear structure, New-York-London, 1970, p.606.
3. *B.B. Wojtsekhowski et al.* Izv. AN SSSR (ser.fiz.), 42 (1978) 2413.
4. *B.B.Wojtsekhowski et al.* Pis'ma ZhETF, 29 (1979) 105.
5. *B.B. Wojtsekhowski et al.* Pis'ma ZhETF, 35 (1982) 299.
6. *D.M. Nikolenko et al.* Nucl. Phys. A446, (1985) 393c.
7. *V.F.Dmitriev et al.* Phys. Lett. 157B, (1985) 143.
8. *D.M. Nikolenko et al.* Abstracts of the invited talks and contributed papers at 11-th Europhysics Divisional Conf. Paris, July 1-5, 1985, p.242(F8), p.244(F9), p.246(F10).
9. *D.M. Nikolenko et al.* Nucl. Phys. A446 (1985) 393c.
10. *B.B. Wojtsekhowski et al.* Pis'ma ZhETF, 43 (1986) 567.
11. *V.F. Dmitriev et al.* Nucl. Phys. A464, (1987) 237.
12. *M.V. Mostovoj et al.* Physics Letters B, 188 (1987) 181.
13. *B.B. Wojtsekhowski et al.* Yad. Fiz., vol. 48 (1988) 6.
14. *R. Gilman et al.* Phys.Rev.Letters, 65 (1990) 1733.
15. *T.W. Donnelly.* Proceedings of the workshop on Electronuclear Physics with Internal Targets, SLAC, January 5-8 8, 1987, p.28.

16. *A.I. L'vov et al.* Preprint INP 91-24, Novosibirsk 1991.
17. *A.M. Sandorfi et al.* Phys.Rev.Letters 45 (1980) 1615.
18. *B.B. Wojtsekhowski et al.* Preprint INP 85-41, Novosibirsk 1985.
19. *A.A. Polunin and Yu.M. Shatunov.* Preprint INP 82-16, Novosibirsk 1982.
20. *I.A. Koop and Yu.M. Shatunov.* "The Spin Procession Tune Spread in the Storage Ring", 1-st European Accelerator Conference, Rome 1988.
21. *D. Drechsel and L. Taitor.* Phys. Lett. 148B (1984) 413.
22. *E. Mazzucato et al.* 57 (1986) 3144.
23. *R. Beck et al.* Phys. Rev. Lett. 65 (1990) 1841.
24. *T.W. Donnelly* **and** *A.S. Raskin.* Annals of Physics, 169 (1986) 247.